DESIGN OF A HALE UAV FOR ATMOSPHERIC IMAGING

Victor Nan Fernandez-Ayala[1], László Vimláti[1], Andreu Matoses Gimenez[1], Helena Delmotte[1], Mykola Ivchenko[1] & Raffaello Mariani[1]

[1]KTH Royal Institute of Technology, Stockholm, Sweden

Abstract

Optical phenomena in the upper atmosphere, such as northern lights, airglow, noctilucent clouds and thunderstorm-related transient luminous phenomena reveal the complex processes coupling different layers of the atmosphere and the near earth space. Bad weather and lighting conditions, as well as geographical constraints, limit the possibilities of ground based imaging. Therefore, an autonomous high altitude long endurance (*HALE*) fixed-wing unmanned aerial vehicle (*UAV*) is proposed for atmospheric imaging, as a joint student-driven research project between the Aeronautics and Vehicle Engineering- and the Space and Plasma Physics departments at KTH Royal Institute of Technology. The Autonomous Light Platform for High Altitude atmospheric imaging (*ALPHA*) is specifically designed for operations in the environmentally harsh conditions found in Arctic nighttime.

This paper presents the conceptual design phase of the aircraft, as well as the initial manufacturing and flight testing methodology of a half-scale prototype.

Keywords: HALE UAV, conceptual design, flight testing, prototype manufacturing, atmospheric imaging

1. Introduction

High altitude long endurance airplanes and UAVs have recently seen a sharp increase in interest [1]. Due to their low cost, simplicity and operational flexibility, UAVs have served as useful platforms for a number of different applications. In addition, the advance of computational technologies and their wide availability have further enabled the design and autonomous control of such aircraft.

The purpose of the development of the ALPHA is to provide a versatile and modular UAV platform for atmospheric research with optical methods. The platform shall support above-cloud, low zenith-angle imaging for extended periods of time in remote locations, in particular during nighttime. Auroras, sprites, blue jets and noctilucent clouds all happen at high altitudes far above the troposphere. In good conditions they can be observed from the ground, but clouds, which can reach a maximum altitude between 5 and 15 km, often hinder visibility. ALPHA is intended to solve this issue, designed to fly in the Arctic at night in cold and low density air. This research project was initiated by the Aeronautics and Vehicle Engineering- and the Space and Plasma Physics departments at KTH Royal Institute of Technology.

The main requirements were that cruise altitude shall be up to 15 km, with a velocity reaching up to 40 m/s while using an electric propulsion system. The design needed to incorporate a flat area on the upper surface of the fuselage featuring a window for optical access. Furthermore, it had to be constituted of maximum 1 m long parts for transportation purposes. The maximum take-off mass of 7 kg, with a combined payload and battery mass not exceeding 3.5 kg, was also specified. Soft requirements were imposed on the design to utilize a conventional aircraft configuration and to achieve a flexible payload modularity for versatility and ease-of-use, as well as an endurance of up to 6 h.
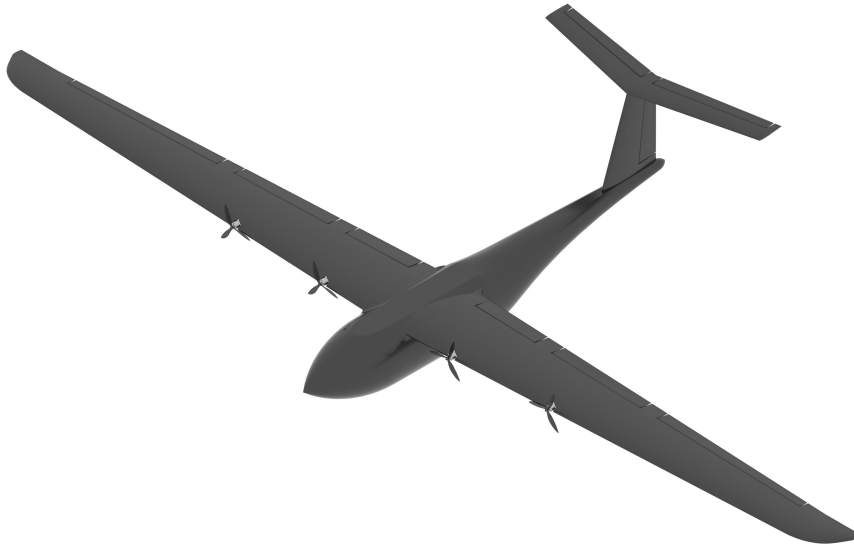
Figure 1 – Current final design of the ALPHA.

Throughout this paper, conventional aircraft design methodologies together with some newer tools, have been implemented to develop an optimal aircraft frame for the stated mission. Additionally, a detailed flight testing procedure to validate performance and the aerodynamic analysis is described in combination with the manufacturing process for a half-scale prototype used for such testing.

2. Conceptual Design

The conceptual design was started with an initial sizing step, involving empirical formulae [2], to obtain early mass and aerodynamic properties that defined the first design. This initial sizing was influenced by the geometry of already existing HALE aircraft [3], and lead to the formulation of a set of aerodynamic and mass parameters, such as the chord and the battery masses required to complete the mission. The main geometric parameters of the wing are presented in Table 1.

Table 1 – A selection of geometry parameters for the main wing from the initial sizing step.

Variable:	b [m]	c_r [m]	c_t [m]	λ	S [m^2]	AR
Value:	4.24	0.40	0.20	0.50	1.296	13.87

Another important aspect that required sizing were the control surfaces, specifically the ones on the wing. During the early stages of the development, three control surfaces were selected: flaps, flaperons and ailerons. Flaps are used to decrease the stall speed for landings as well as to extend the ceiling altitude by a small margin that might be useful when trying to avoid clouds. Flaperons are controlled by a linear combination of the flap and the aileron deflections, aiding the flaps during taking off or landing and the ailerons at high altitudes where the density is lower and the moments generated would also be smaller. Lastly, ailerons give the aircraft control over the roll axis. All the control surfaces on the wing are 20% of the chord, while the ones in the tail are 35% of the chord, based on Raymer's approach [2].

The last step in the early development phase of the ALPHA is the selection of the number of motors and their placement. In this case, four brushless electric motors of around 1 kg of static thrust each at sea level were selected to be placed in the sections between the middle of the flaperons and flaps as shown in Figure 1. With four motors enough redundancy can be achieved, without increasing the power consumption and weight of the electronics due to the extra losses and components needed.

Once a baseline design was established, the initial aerodynamic analysis involved an airfoil selection step that included evaluation of both experimental and simple XFOIL [4] simulation data, through the open source software *XFLR5*. The Reynolds number was estimated to approximately 2.5×10^5 for the cruise conditions at 15 km altitude, which required the airfoil selection to focus primarily on low-Reynolds number airfoils. The selection process was based on the work of Selig [5], where the author's recommendations and experimental results were utilized to formulate a list of possible airfoils that were later analysed using XFLR5. The airfoil analysis highlighted two candidates: SD7080 and SA7035, which are shown together with the aerodynamic analysis using XFLR5 in Figure 2.
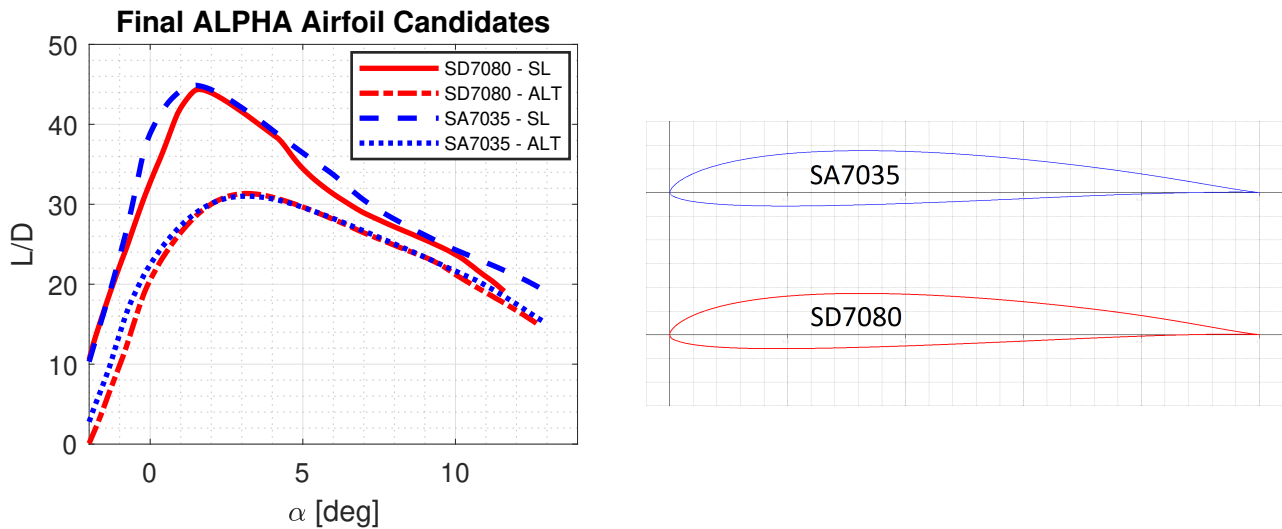
Final ALPHA Airfoil Candidates

Figure 2 – Aerodynamic efficiency analysis for the final airfoil candidates for ALPHA using XFLR5 (left) and drawing of the SA7035 airfoil (right, top) and SD7080 airfoil (right, bottom).

Preliminary numerical data showed that the SA7035 airfoil was more suitable for the cruise condition, while experimental data by Selig and Lyon [5, 6] showed that SD7080 had superior performance in the mid-lift region of the drag polar for even lower Reynolds numbers. The SD7080 airfoil was ultimately chosen, as the available wind tunnel data was deemed more accurate than the XFOIL analysis which was developed for high Reynolds number flows. The commonly used NACA 0009 was selected for the vertical and horizontal tail due to its low drag among symmetric airfoils.

Once the airfoils were selected, the next phase of the design process was initiated, by commencing a simple aerodynamic analysis on the wing and tail configuration from the initial sizing step using XFLR5, to give an early performance indication. The placement and size of the tail section were optimized to obtain the desired trim point and reduced drag. As XFLR5 does not support accurate modelling of the fuselage, its effect on the drag of the ALPHA was introduced as an added external drag coefficient of $C_{D,f} = 0.009$, obtained from a preliminary numerical simulation of a simplified fuselage. This result was taken as the reference case for the more extensive Computational Fluid Dynamics (*CFD*) phase, using the ANSYS Fluent solver [7].

The CFD simulations of the ALPHA were divided into three main parts: analysis of the wing only, of the fuselage and tail only, and of the full configuration. The first two sets of simulations were only performed at sea level and altitude flight at zero and three degrees angle of attack, as these conditions are those of highest interest for the fulfillment of the mission requirements of the ALPHA. Finally, simulations of the full configuration were conducted on a range of angles of attack, from zero to twelve degrees, in order to obtain a more extensive prediction of the aerodynamic properties. Results were obtained by solving the Reynolds Averaged Navier Stokes (*RANS*) equations, applying the widely used k-ω SST turbulence model [8] with full resolution of the viscous sublayer using nominal y$^+$ of 1, as recommended for low-Reynolds number flows [9].

These computations were performed on a computer with 128GB RAM and an AMD Ryzen 9 3900XT 12-core processor. The different flight altitudes were introduced in the simulations by changing the density and the viscosity of the air, which was modelled as an incompressible, ideal gas. A rectangular computational domain was used, with up to four bodies of influence, where the computational mesh element sizes were gradually decreased closer to the aircraft. The grid independence study showing small variation and the sufficient y^+ distribution along the fuselage and wings for the cruise case are presented in Figures 3 and 4 respectively. Due to the limited computational capacity the maximum grid size was approximately 10 million nodes, which prevented finer grids.
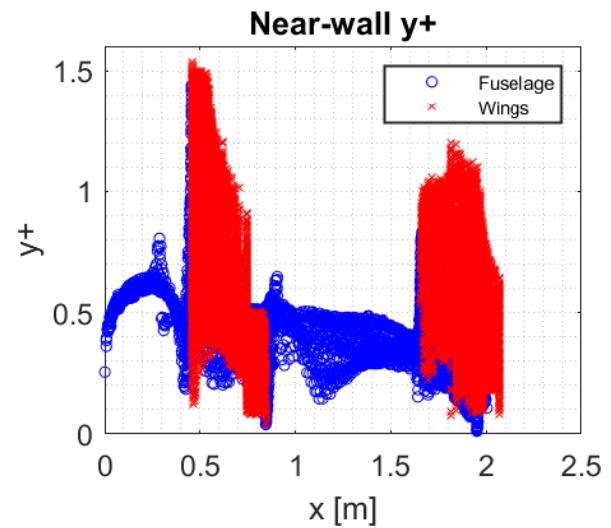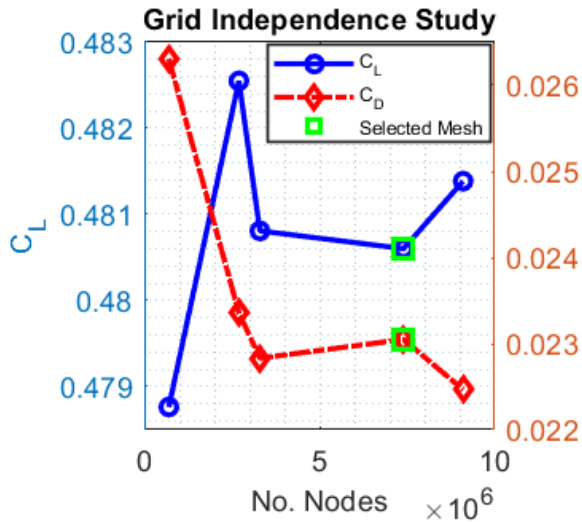

Figure 3 – Grid independence study, final mesh contained 7.6mil nodes.

Figure 4 – Near-wall y+ presented alongside the longitudinal coordinate of each node.

Further design iterations were performed, aimed at optimizing the aerodynamic efficiency of the fuselage and wing, focusing on simulation of different configurations. Simulations were run only for target cruise conditions, to minimize the computational cost. It was found that a sharp nose shape in combination with raked wingtip extensions were the most efficient configuration. These extensions were added to redistribute the lift across the entire wing and redirect the wingtip vortices further outboard and aft of the wing. This effect is shown in Figure 5, for 3° angle of attack at altitude, which resulted in a 1.75% increase in aerodynamic efficiency.
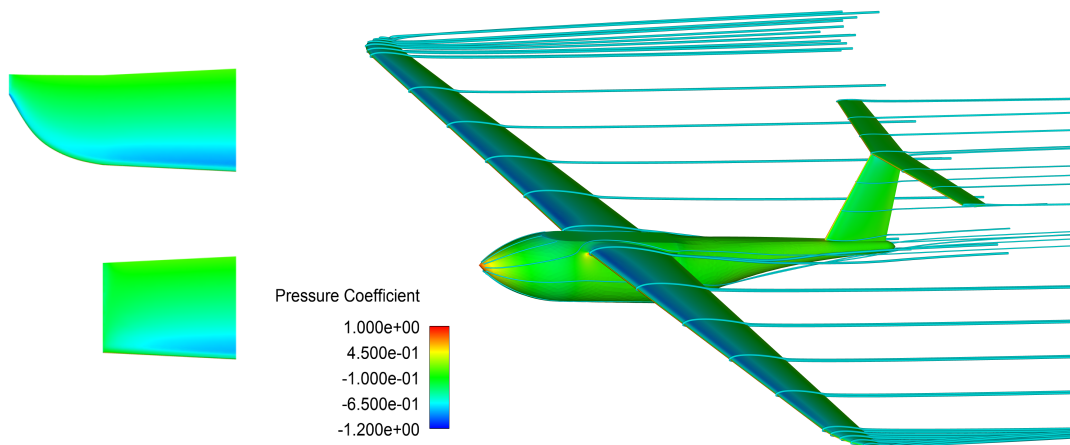

Figure 5 – Pressure contour of ALPHA. Comparison of wing tip versions (left) and streamlines around full configuration (right).

4

Three different types of tail configurations were evaluated through CFD simulations using the full configuration at cruise condition. These were a conventional tail, T- and H-tail. The T-tail configuration, shown in Figure 1, was selected since it produced a 12.4% increase in aerodynamic efficiency and was found to be most simple to manufacture among the cases considered. The resulting final design of ALPHA had a wingspan of 4.64 m and a total length of 2 m.

Simulations were performed for a range of angles of attack, at both sea level and altitude, and compared to the initial configuration. The aerodynamic performance is presented in Figure 6 for the final aircraft configuration is shown in Figure 7.
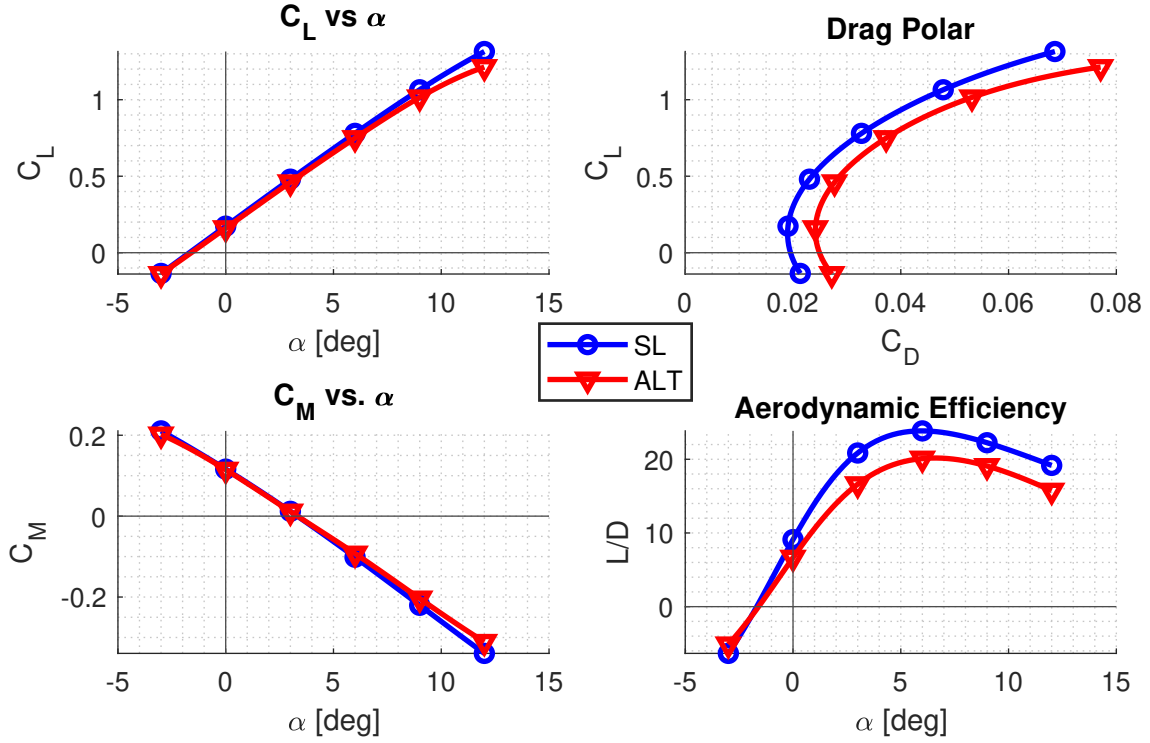

Figure 6 – Simulation results at sea level and at cruise conditions for the final ALPHA design.

Based on the final aerodynamic performance, the endurance was compared to the mission requirements. This was estimated as shown in Raymer [2] using:

$$Endurance_{cruise} = \frac{E_{spec}}{g} MF_{bat,cruise} \, \eta_{tot} \frac{L/D}{V} \tag{1}$$

where $V = 40$ m/s, the efficiency $\eta_{tot} = 0.8$, MF is the mass fraction of the battery and $E_{spec} = 260$ Wh/kg is the specific energy of sample Lithium-Ion batteries, which are one of the most efficient and widely available [10] types of batteries. The loitering endurance prediction was determined to be 3 h 10 min, which is below the initial 6 h requirement. In order to achieve the expected mission endurance, the aircraft will be lifted by a helium balloon to an altitude of 20-25km, at which point the UAV would be released and controlled powered gliding would be implemented to attain the desired altitude while taking advantage of regenerating braking to recharge the batteries. Consequently, the flight time would be extended by an extra 1-3 h, based on [2]:

$$E_{glide} = r \frac{\Delta h}{V \sin \frac{D}{L}} \tag{2}$$

where Δh is the extra altitude after 15 km and $r \geq 1$ is the regenerative braking extension to the gliding time.
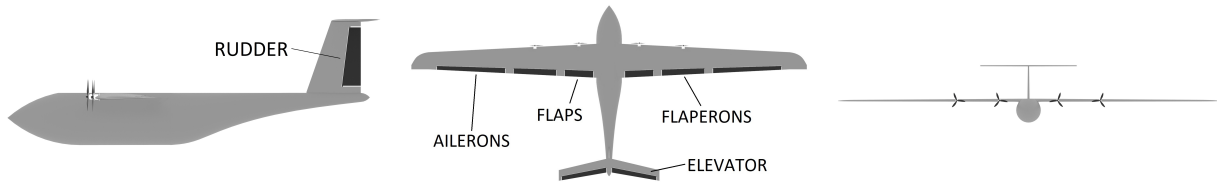
Figure 7 – Side, top and front view of the final design of the ALPHA .

3. Sub-Scale Prototype

A half-scale prototype is being manufactured to benchmark the simulated aerodynamic performance and test stability in addition to the flight control systems. The prototype will also test the customized control routines for the landing and balloon release. Additionally, it will be used for further fine tuning of the design and resolving integration issues before flying the more complex full scale aircraft.

To properly size the power plant for the half-scale prototype, an empirical approximation of the dynamic thrust was used, calibrated on experimental static thrust tests of a brushless motor *EMax ECO II 2207 2400KV* with 5x4.3x3 propellers Figure 8. According to [11], the method performs well for low speeds close to static thrust measurements, but poorly for zero thrust speed estimation, under-predicting this maximum speed up to 30% when compared to measurements of similar power plants tested in wind tunnels. Comparing dynamic thrust for a given flight speed and drag based on the CFD simulations showed that speeds close to the full-scale cruise speed can be achieved with the configuration of four propellers, see point A Figure 9 and not much improvement is attained by the six propeller configuration, point B. Results also show that a more accurate dynamic thrust approximation using experimental data is needed to properly evaluate the power plant.

Figure 8 – Motor *EMax ECO II 2207 2400KV* with propellers of 5" radius, 4.3" pitch and 3 blades (5x4.3x3) mounted in the thrust bench used for the static thrust tests.
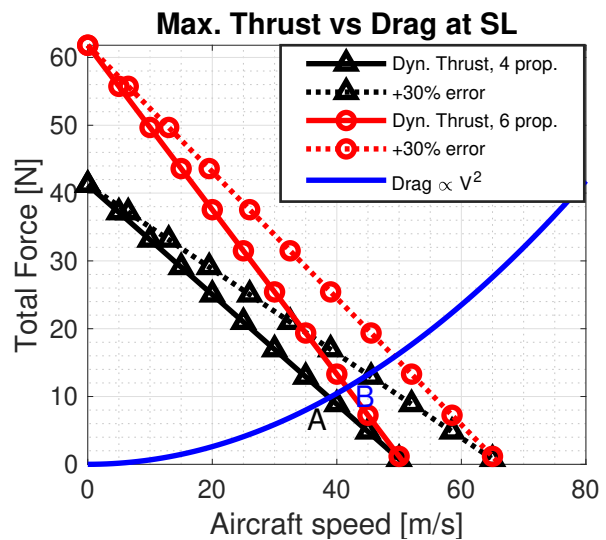

Figure 9 – Dynamic thrust approximation against drag for 4 and 6 motors used in the half scale UAV. The intersection of $T = D$ named A, B respectively shows maximum reachable speed.

3.1 Subscale Flight Testing

The "Test Campaign", a sequence of flight tests, was designed to determine flight, aerodynamic and control performance. The campaign aims at providing a systematic approach to testing and fine tuning the control algorithms which will be used as a base for the control of the full scale UAV. Emphasis was put on the methodology in order to standardize flight test procedures for future design iterations and to significantly reduce testing time [12].

Flight mechanics and control tests focus on verifying the stability of the aircraft during flight and the proper functioning of the control algorithms. The tests to be conducted in this group are:

1. Induction of natural modes on flight, which assesses general dynamic stability of the aircraft [13]. This is done by a scripted sequence of control inputs, while the control feedback is deactivated for a short time. Additionally the ability of the control system to stabilize the phugoid and spiral responses need to be tested as preliminary analysis showed that although slow, both modes are naturally unstable Table 2.

Table 2 – Natural mode responses for the half-scale simplified dynamic model from XFLR5.

Natural mode		Characteristics	
Longitudinal	Phugoid	Frequency: 0.12 Hz	Damping ratio: 0
	Short period	Frequency: 2.39 Hz	Damping ratio: 0.71
	Spiral	Time to double amplitude: 5.87 s	
Lateral	Roll damping	Time to halve = 0.02 s	
	Dutch roll	Frequency: 0.82 Hz	Damping ratio: 0.32

2. Forced input dynamic responses. These tests evaluate the aircraft response to specific deflections of the control surfaces. The different types of control deflections to test are impulse, step and ramp inputs by means of scripted actioning during flight. Each control surface is tested individually. Data obtained can be used for performing system identification and obtaining a mathematical model of the system dynamics [14] for further optimization of the controller.

3. Recovery tests. These tests asses the capability of the aircraft to recover steady flight conditions after conditions outside the operational range envelope. Three tests are planned: dive tests, recovery from stall, and recovery from balloon take off.

   For the recovery from balloon take off, several preliminary tests are planned. First in a virtual flight simulator to verify the proper behaviour of the control routine; then by releasing a model of the aircraft by hand, pitch down, from a tall structure and finally during flight at a safe altitude, by performing a pronounced dive.

4. Autonomous flight capabilities. Due to legal and physical constraints, bounds in the allowed flight area will be imposed during flight. Additionally, planned way-points and trajectories need to be followed by the control system. These tests aim to verify the accuracy with which the controller is able to follow said constraints.

Subscale aerodynamic tests aim to benchmark and validate the results obtained through CFD analysis. They will also provide realistic information about the limits in performance.

1. Stall conditions. These tests consist in finding the maximum angles of attack for different velocities as well as flight configurations (flaps on/off). These tests also give a qualitative analysis in the nature and severity of the stall.

2. Approximation of C_L and C_D. Equilibrium of forces is assumed in a controlled steady level flight and lift and drag can be approximated as weight and thrust respectively [15]. The quality of the C_D approximation is directly related to the quality of the approximated dynamic thrust, reiterating the importance of the proper calibration of the model used in Figure 9. The test is repeated several times in different flight directions to obtain a statistical average of the coefficients.

3.2 Half-Scale Manufacturing

The manufacturing of the half-scale prototype was divided in two main parts: the structural design and the manufacturing of the prototype. The first step of the structural design was to determine the type of structure and materials used for the prototype. The second step was the design of the complete assembly accommodating more practical consideration such as joints, placement of the electronics component, landing gear etc. The manufacturing of the prototype started in parallel to the design with some testing of the manufacturing processes.

The conceptual design of the structure was driven by two given requirements: a part shall not be longer than 1 m and the prototype shall be easily assembled and dismantled on site. The priority was to ensure an accurate representation of the full scale UAV's shell. In particular the leading edge shape was to be of high accuracy for aerodynamic considerations. Three classic wing configurations were considered. The first was a spar-rib structure with film covering. While very light, this structure does not provide the exact expected leading edge shape in between the ribs. The second was a composite wing, using a carbon fiber epoxy matrix laminate for example. This structures does not only guarantee a light and stiff wing, but also an excellent leading shape. However, it requires specific equipment and installation to manufacture that were not accessible at the time. The third configuration studied was a foam body as foam is a classic material for UAVs of this scale and provides a good leading edge and surface finish. To obtain an accurate shape of the wing two machines can be used: a foam laser cutter or a CNC milling machine. Thanks to a ready availability of a CNC machine, this solution was chosen as the final one. For stiffness purposes, off-the-shelf carbon fiber spars were added to the structure. Furthermore, to improve the shear strength of the structure as well as protecting the foam from dents, a glass fiber tape was chosen to cover the wings and tail.

A comparison was made of different samples of structural foam on three criteria: density, surface finish after manufacturing, ease of supply. The foam types considered were EPP (40 kg/m^3), XPS (30 kg/m^3) and closed cell PVC (40 kg/m^3). The same portion of the wing was manufactured with the three foams using a CNC machine as shown in Figure 10.

Figure 10 – Wing sample for foam testing - From back to front EPP, PVC and XPS foam.
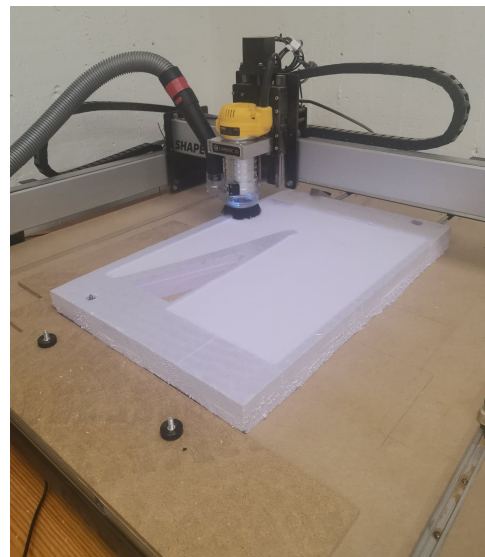

Figure 11 – CNC machine while manufacturing a part of the fuselage.

XPS had in overall the best surface finish, EPS provided the best result on the thin trailing edge and PVC came last on both accounts. However, procurement of EPS foam was not straightforward and therefore the XPS solution was chosen. A wing manufactured using XPS is shown in Figure 12.
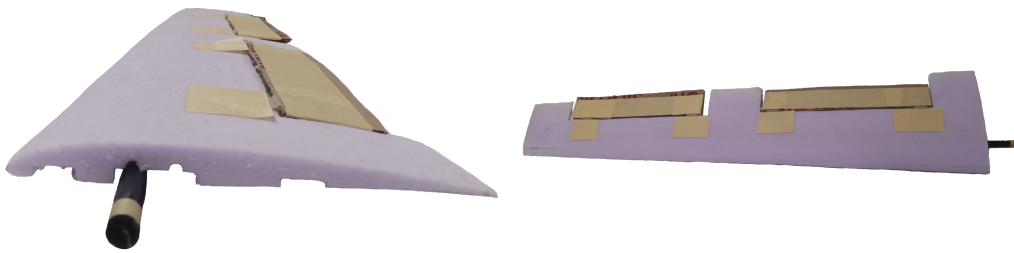
Figure 12 – Wing mock-up, side view (left) and top view (right).

Once the structure and materials had been chosen, the modelling of the prototype began. With a length slightly less than 1 m the fuselage of the UAV did not require to be built in two sections. However, because of a 2.32 m wingspan for the half-scale prototype, the wings needed to be manufactured in at least 3 parts to meet the transport requirement. Sectioning of the wing was determined by the location of the control surfaces on the wing. As shown by the section A-A in in Figure 13, the separation was positioned in between the two first ailerons to facilitate the mechanical and electronic assembly for each wing. Indeed since the wings need to be modular, the separation does not only concern the body of the wing but also the cables for the electronics. Therefore, a joint between each part of the wings was designed to help carry the torsional loads and to host the locking mechanism enabling the assembly and disassembly of the wings. For the motors, holders were designed to be connected to the spars as shown in Figure 13.
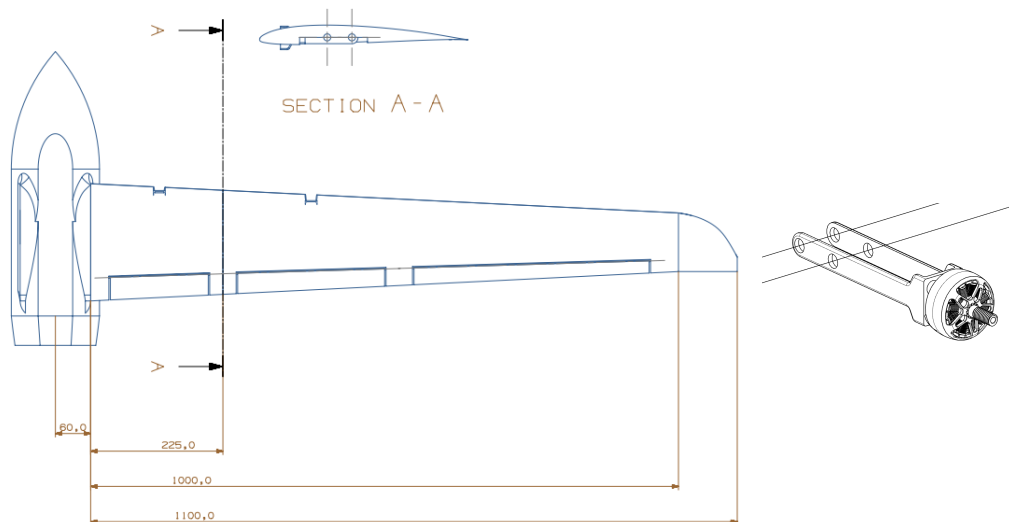

Figure 13 – Drawing of the right wing and fuselage (left) and the motor holder (right). Section A-A is the plane of junction of the wing.

Finally, placement of the electronics were also taken into consideration with spaces carved in the wings, fuselage and tail for wires. The inside of the fuselage was designed to host the battery, flight controller, GPS, antennas and other necessary equipment as shown in Figure 14. The manufacturing tests previously mentioned highlighted new constrains in the design due to the limitation of the CNC machine shown in Figure 11. The working area is 81.9x77.2 cm with a maximum range of 9.19 cm in thickness without tool. Thus, the model needed to be divided in manufacturable parts for which toolpaths would be made. To ensure a precise work, the model of the UAV is seperated in parts that don't exceed the dimensions 75x70x5 cm. Individual parts are to be glued as a single body as necessary. Model separation for manufacturing is shown in Figure 14.
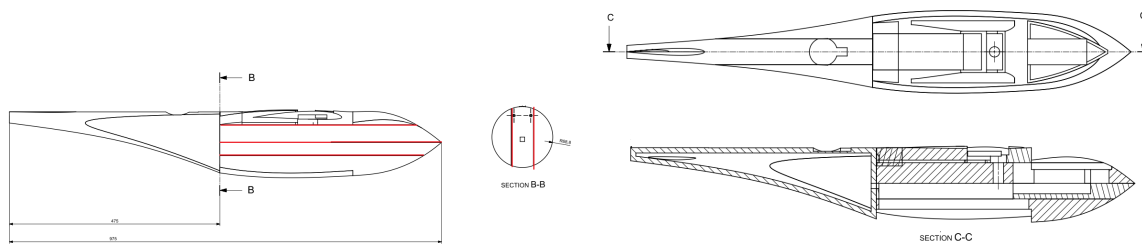
Figure 14 – Fuselage body with (left) and without (right) lids. Red lines indicates manufacturing cutting planes.

4. Conclusion

In this paper, the design of a HALE UAV for atmospheric research with optical methods has been studied. The starting point was the specification of requirements, which was followed by the initial sizing, the aerodynamic analysis and ended with the flight testing and manufacturing of a half-scale prototype. Key results and data has been shown thorough the paper with both plots of aerodynamic properties, renders and technical drawings, which demonstrate the feasibility of the design for the intended mission.

5. Copyright Statement

The authors confirm that they, and/or their company or organization, hold copyright on all of the original material included in this paper. The authors also confirm that they have obtained permission, from the copyright holder of any third party material included in this paper, to publish it as part of their paper. The authors confirm that they give permission, or have obtained permission from the copyright holder of this paper, for the publication and distribution of this paper as part of the ICAS proceedings or as individual off-prints from the proceedings.

References

[1] Goraj Z, Frydrychewicz A and Świtkiewicz R et. al. High altitude long endurance unmanned aerial vehicle of a new generation - A design challenge for a low cost, reliable and high performance aircraft. *Bulletin of the Polish Academy of Sciences, Technical Sciences*, Vol. 52, No. 3, pp 173-194, 2004.

[2] Raymer D.P. *Aircraft Design: A Conceptual Approach*. 6th edition, AIAA Educational Series, 2018.

[3] Merlin P.W, *Unlimited Horizons Design and Development of the U-2*. National Aeronautics and Space Administration, 2015.

[4] Drela M, XFOIL: An Analysis and Design System for Low Reynolds Number Airfoils. *Low Reynolds Number Aerodynamics*, Notre Dame, Indiana, Vol. 54, pp 1-12, 1989.

[5] Selig M.S and Donovan J.F and Fraser D.B. *Airfoils at Low Speeds*. H.A. Stokely, 1989.

[6] Lyon C.A and Broeren A.P and Giguère P et.al. *Summary of Low Speed Airfoil Data - Volume 3*, SoarTech Publications, 1997.

[7] Ansys®, Fluent 2020 R2, Academic Release.

[8] Menter F.R. Two-equation eddy-viscosity turbulence models for engineering applications. *AIAA Journal*, Vol. 32, No. 8, pp. 1598-1605, 1994.

[9] Ansys®, Fluent Theory Guide Release 12.0, Section 4.12.1, 2009.

[10] Panasonic, Panasonic 18650 Li-ion Cells. [Online]. Available: `https://www.greencarcongress.com/2009/12/panasonic-20091225.html`

[11] G. Staples. Propeller Static & Dynamic Thrust Calculation. [Online]. Available: `https://www.electricrcaircraftguy.com/2014/04/propeller-static-dynamic-thrust-equation-background.html` (28/05/2022)

[12] A. Sobron. *On Subscale Flight Testing : Applications in Aircraft Conceptual Design*, Linköping University Electronic Press, 2018.

[13] R. C. Nelson. *Flight stability and automatic control*. Boston, Massachusetts, WCB/McGraw Hill, 1998.

[14] R. Larsson. *Flight Test System Identification*. PhD dissertation, Linköping University Electronic Press, Linköping, 2019.

[15] D. P. Bergmann, J. Denzel, O. Pfeifle, S. Notter, W. Fichter, and A. Strohmayer. In-flight Lift and Drag Estimation of an Unmanned Propeller-Driven Aircraft. *Aerospace*, Vol. 8, No. 2, p 43, 2021.